

SCIENTIFIC REPORTS



OPEN

High-power graphene mode-locked Tm/Ho co-doped fiber laser with evanescent field interaction

Xiaohui Li^{1,4}, Xuechao Yu¹, Zhipei Sun², Zhiyu Yan¹, Biao Sun¹, Yuanbing Cheng¹, Xia Yu³, Ying Zhang³ & Qi Jie Wang¹

Received: 14 June 2015

Accepted: 16 October 2015

Published: 16 November 2015

Mid-infrared ultrafast fiber lasers are valuable for various applications, including chemical and biomedical sensing, material processing and military applications. Here, we report all-fiber high-power graphene mode-locked Tm/Ho co-doped fiber laser at long wavelength with evanescent field interaction. Ultrafast pulses up to 7.8 MHz are generated at a center wavelength of 1879.4 nm, with a pulse width of 4.7 ps. A graphene absorber integrated with a side-polished fiber can increase the damage threshold significantly. Harmonics mode-locking can be obtained till to the 21th harmonics at a pump power of above 500 mW. By using one stage amplifier in the anomalous dispersion regime, the laser can be amplified up to 450 mW and the narrowest pulse duration of 1.4 ps can be obtained simultaneously. Our work paves the way to graphene Tm/Ho co-doped mode-locked all-fiber master oscillator power amplifiers as potentially efficient and economic laser sources for high-power laser applications, such as special material processing and nonlinear optical studies.

Long-wavelength ($>1.55\ \mu\text{m}$) ultrafast lasers can potentially be applied in various applications, such as free-space optical communication due to atmospheric transparency window, molecular spectroscopy, medical diagnostics, laser surgery, long-range radar, and gas detection¹. They can also be applied in high-efficient industrial material processing of various special materials, such as plastics, glasses, and leather because of their strong absorption in the mid-infrared range²⁻⁴. Compared to the conventional solid-state laser counterpart, fiber laser recently attracts considerable interests due to its alignment-free structure, compactness, efficient heat dissipation, and superior output performance (such as high beam quality, environmental stability, and flexible output).

Mode locking is the most typical approach to generate ultrashort pulses. Various methods have been reported to achieve mode locking: Nonlinear polarization rotation (NPR) is the one of the most commonly used methods for fiber laser mode locking, which have been studied for many years⁵. Other methods, such as nonlinear amplifying loop mirror (NALM), nonlinear optical loop mirror (NOLM) etc. have also been utilized to achieve mode locking⁶⁻⁸. Different materials, with ultrafast response time, have also been studied to achieve mode locking. Semiconductor saturable absorber mirror (SESAM) has been used as a type of saturable absorber (SA) for quite a long time^{9,10}. However, it has some drawbacks, such as complex fabrication and packaging, low damaged threshold, high cost. Recently, single-wall carbon nanotubes (SWNT) and graphene¹¹⁻¹⁶, have also been demonstrated as promising SAs for ultrafast pulse generation¹⁷⁻¹⁹. In particular, graphene has shown excellent performance to generate ultrashort pulses, such as broadband operation^{20,21}, ultrafast recovery time¹², ease of fabrication, and integration into all-fiber structure^{19,22}. Diverse fabrication methods have also been utilized for graphene

¹Center for OptoElectronics and Biophotonics, School of Electrical and Electronic Engineering & The Photonics Institute, Nanyang Technological University, 50 Nanyang Ave., 639798, Singapore. ²Department of Micro- and Nanosciences, Aalto University, PO Box 13500, FI-00076 Aalto, Finland. ³Singapore Institute of Manufacturing Technology, 71 Nanyang Drive, 638075 Singapore. ⁴School of Physics and Information Technology, Shaanxi Normal University, Xi'an 710062, P.R. China. Correspondence and requests for materials should be addressed to X.Y. (email: xyu@SIMTech.a-star.edu.sg) or Q.J.W. (email: qjwang@ntu.edu.sg)

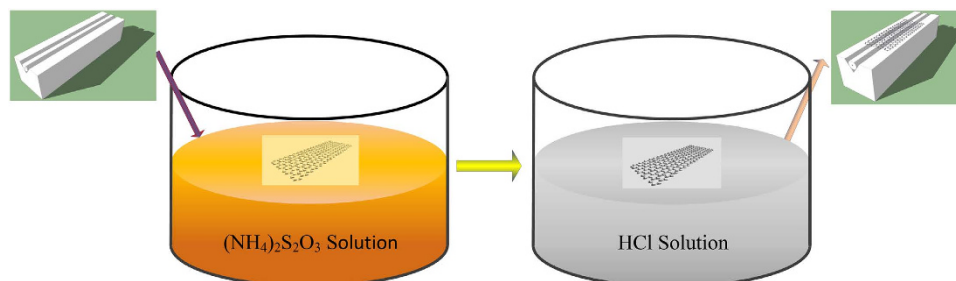


Figure 1. Transferred method for preparing graphene SA. The left part is schematics of the side-polished fiber without graphene. The MCVD grown graphene is dissolved in an aqueous $(\text{NH}_4)_2\text{S}_2\text{O}_3$ solution. The cleaned PMMA/graphene film is dissolved in 0.5 M HCl solution. The side-polished fiber is put at the bottom of PMMA/graphene film in the breaker to pick up the target. The right part is the side polished fiber with graphene.

saturable absorber fabrication, such as micromechanical cleavage²³, liquid phase exfoliation (LPE)²⁴, chemical-vapor-deposition (CVD)^{25,26}, and carbon segregation from silicon carbide^{27,28}. Various integration methods have been demonstrated for graphene-based all-fiber device integration: such as directly sandwiched between two-fiber ends²⁹, sprayed on the glass³⁰, or the side polished fibers³¹.

In order to generate ultrashort pulse at wavelength above $1.55\ \mu\text{m}$ and even up to $3.9\ \mu\text{m}$ ^{32,33}, erbium (Er), thulium (Tm), holmium (Ho), or Tm/Ho-co-doped active fibers are utilized to offer appropriate gain region for fiber laser applications. Very recently, graphene ultrafast fiber lasers have been demonstrated at the mid-infrared spectral range. Tm-doped mode-locked fiber lasers based on graphene or multi-layer graphene-polymer composite^{34–38}, graphene oxide³¹, have been demonstrated. High pulse energy Tm/Ho-co-doped fiber laser has also been demonstrated³⁹. However, most of the power level is limited to several mW levels and the peak power is less than hundreds of Watt, limiting their applications.

In this paper, we utilize the side-polished fiber together with graphene grown by CVD method to achieve mode locking in a Tm/Ho co-doped ring fiber laser. It is demonstrated that mode locking can be obtained at a center wavelength of 1879.4 nm, spectral bandwidth of 1.8 nm, and pulse width of about 4.7 ps. High-order harmonic mode locking (up to 164.6 MHz) can be obtained with the increase of pump power. After we use a Tm-doped fiber amplifier (TDFA) to boost the output power, the maximum output power is $\sim 450\ \text{mW}$, corresponding to the peak power of about 9.7 kW. Our results shows graphene all-fiber Tm/Ho co-doped mode-locked fiber laser with single mode output and high peak power. These unique properties enable the advantages of compactness, good beam quality and high power output, which make them potential candidates in the molecular spectroscopy, nonlinear frequency conversion, and laser surgery applications.

Results

CVD grown single layer graphene (SLG) ($\sim 20 \times 20\ \text{mm}^2$, Graphene Supermarket) is transferred onto a side-polished fiber embedded in a glass plate by a modified transfer process. Figure 1 shows the schematic of the transferred processes. As-fabricated SLG on the copper is spin-coated with poly (methyl methacrylate) (PMMA, average $M_w \sim 996000$ by GPC, Sigma Aldrich, dissolved in chlorobenzene with a concentration of 50 mg/mL), which is then cured at $110\ ^\circ\text{C}$ for 10 min. The underneath Cu foil is then dissolved in an aqueous $(\text{NH}_4)_2\text{S}_2\text{O}_3$ solution (10%). The remaining PMMA/graphene film is cleaned by repeatedly dipping it in deionized water, and then a 0.5 M HCl bath for 5–10 min. Then, the PMMA/graphene film is picked up through the target side-polished fiber. After drying in the ambient condition, some PMMA solution is dropped onto the side-polished fiber to dissolve the pre-coated PMMA and flatten out wrinkles on the graphene. The PMMA is then dissolved in acetone, leaving SLG on glass with side polished fiber.

After transfer, the graphene on the side-polished fiber was characterized by Raman spectroscopy (under 532 nm excitation) and absorption microscopy. A representative Raman spectrum of the transferred graphene on side-polished fiber is shown in Fig. 2(a). 2D peak has a single Lorentzian shape. The ratio of G and 2D Raman peaks (I_G/I_{2D}) is 0.54, which is recognized as intrinsic single layer graphene⁴⁰. The negligible D, $D+D''$ and $2D'$ band indicates high quality of CVD SLG⁴¹. The inset shows the microscope image of our transferred graphene on side-polished fiber. The left part of the red-dashed line in the image is with SLG which covers the side-polished fiber. The right part of red-dashed line is without SLG. In addition, we use a home-made broadband Amplified spontaneous emission (ASE) source (from 1700 to 2100 nm) to measure the linear transmittance of the side polished fiber integrated with SLG. The result is shown in Fig. 2(b). The transmittance at 1880 nm is about 40%. The inset of Fig. 2(b) shows the schematic diagram of side-polished fiber covered with SLG SA.

Figure 3 shows the schematic of the proposed fiber laser based on our fiber-integrated graphene SA. The fiber laser is composed of several fiber components, including a 1.5-m-long Tm/Ho co-doped fiber

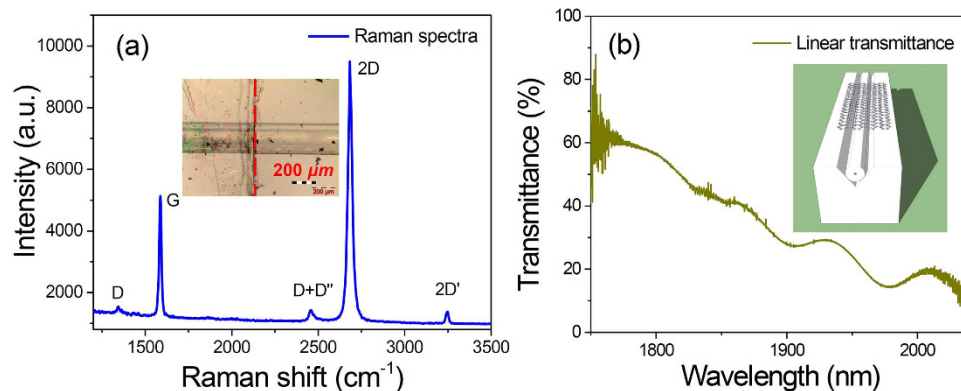


Figure 2. (a) The Raman spectrum of the CVD grown graphene SA device. Inset: the microscope image of our transferred graphene on the side polished fiber with the scalar bar of 200 μm . (b) Linear transmittance of our fiber-integrated graphene saturable absorber. Inset: schematic diagram of a side-polished fiber covered with graphene as a SA device.

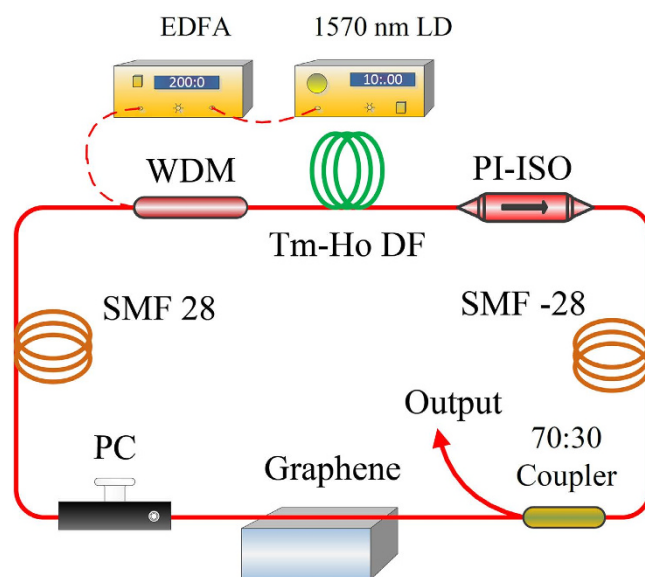


Figure 3. The experimental setup of the Tm/Ho co-doped fiber laser based on side-polished fiber with graphene.

(from CorActive company) with absorption of 137 dB/m at 790 nm, a 1570/1950 wavelength division multiplexing (WDM) coupler, a polarization insensitive isolator (PI-ISO), one polarization controller (PC), a 70:30 optical coupler (OC), and a side-polished fiber covered with SLG. A 1570-nm laser diode with ~ 10 -mW output power amplified with C+L band erbium-doped fiber amplifier (EDFA), which has the capability of amplifying the signal to more than 1 W, is used as pumping source for the laser system. The pulse train is exported from the fiber cavity through 30% port of OC. All the fiber components inside the laser system are fusion spliced, with a total length of about 26.2 m.

When the pump power reaches 371 mW, mode-locking can be self-started. When we decrease the pump power, pulse train can be maintained till 326 mW, which is due to the hysteresis effect⁴². The hysteresis effect in the experiment is identical to other rare earth-doped passively mode-locked fiber lasers, such as Yb-doped fiber laser in the 1- μm region, and Er-doped fiber laser in the 1.5- μm region.

The typical output of the fiber laser (optical spectrum, oscilloscope trace, RF spectrum, and the corresponding autocorrelation trace) is shown in Fig. 4. Figure 4(a) shows the typical spectrum of fiber lasers with a center wavelength of 1879.4 nm. The spontaneous emission hump of single mode Tm/Ho co-doped fiber is located at 1880 nm when the length of the fiber is around 2 m, and thus the maximum gain can be obtained around this wavelength regime. Spectral sideband is observed, indicating that our fiber laser operates in the conventional soliton mode-locking regime. With the increase of the length of Tm/Ho co-doped fiber, the center wavelength can shift to longer wavelength side, which is

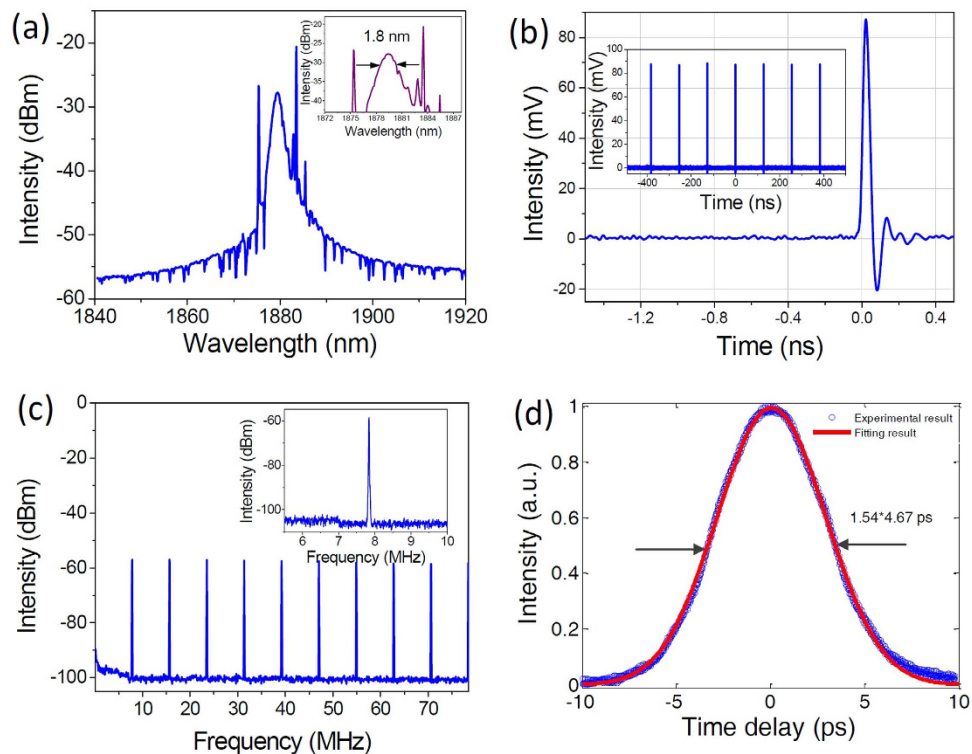


Figure 4. The output characteristics of Tm/Ho co-doped mode-locked fiber laser at the fundamental repetition rate. (a) Output spectrum, inset: the spectral width is about 1.8 nm, (b) single pulse as observed from the high-speed oscilloscope, inset: corresponding pulse train, (c) RF spectra, inset: RF spectra at the fundamental frequency of ~ 7.8 MHz, (d) autocorrelation trace, with pulse width of 4.67 ps.

due to secondary pumping phenomena in an un-pumped active fiber⁴³. The inset of Fig. 4(a) shows the zoom-in spectrum, indicating spectral width of 1.8 nm. Figure 4(b) shows the oscilloscope trace of a single pulse obtained from a high-speed oscilloscope. The inset shows the pulse train with a period of 127.6 ns. Figure 4(c) shows the RF spectra with a span of 78 MHz. Nine frequency peaks can be observed within the range. The inset is the fundamental frequency of ~ 7.8 MHz. Figure 4(d) indicates that the pulse temporal profile is well fitted by a sech^2 profile with a pulse width of 4.67 ps. The corresponding 3-dB spectral width is 1.8 nm, corresponding to a time-bandwidth product (TBP) of about 0.714. The TBP is larger than transform-limited sech^2 pulse, which indicates the pulses are chirped. Compared with Ref. 31, the output of our proposed fiber laser, with a total dispersion of about -1.757 ps^2 , is comparable. The pulse width can be further reduced by controlling the dispersion of the cavity.

With further increasing the pump power, our fiber laser can operate from the fundamental mode locking regime to the high-order harmonic mode-locking regime. Figure 5(a) shows the output power versus the pump power of our Tm/Ho co-doped fiber laser. The slope efficiency is around 4.8% through linear fitting as shown in pink line. Considering the linear loss of around 60% induced by the side-polished fiber with SLG and other components, the slope efficiency is reasonable. Different operation regimes can be achieved under different pump power and are represented by using different colors. ASE regime is from 230 mW to 300 mW represented in the yellow color area. CW and unstable regimes are from 300 mW to 326 mW in blue color area. Fundamental mode locking regime can be obtained from 326 mW to 338.9 mW represented in the red color area. Number “1” is used to represent the fundamental mode locking regimes. High-order mode locking is in above 338.9 mW in green color. Figure 5(b) shows the repetition rate and orders of harmonic mode locking versus pump powers. Through increasing the pump power, the order of the mode locking increases. When the pump power is increased to 517.4 mW, our fiber laser can operate at the 21th harmonics mode locking, which gives an output of 10.1 mW with a repetition rate of 164.6 MHz. Because of the limitation of the damage threshold of the fiber components (500 mW), the pump power are not further increased. Figure 5(c) shows the spectra evolution at the fundamental, 5th, 8th, 11th, 15th, and 21th harmonic mode locking versus the different pump power. Figure 5(d) shows the corresponding pulses-train evolution. Harmonics mode locking state can be partially explained by the soliton energy quantization theory⁴⁴. Due to the soliton energy relocation and the interaction between the multiples solitons per round cavity round trip, the multiples at high pump power will form a special state, which have the equal separation in the fiber cavities, i.e. harmonics mode locking.

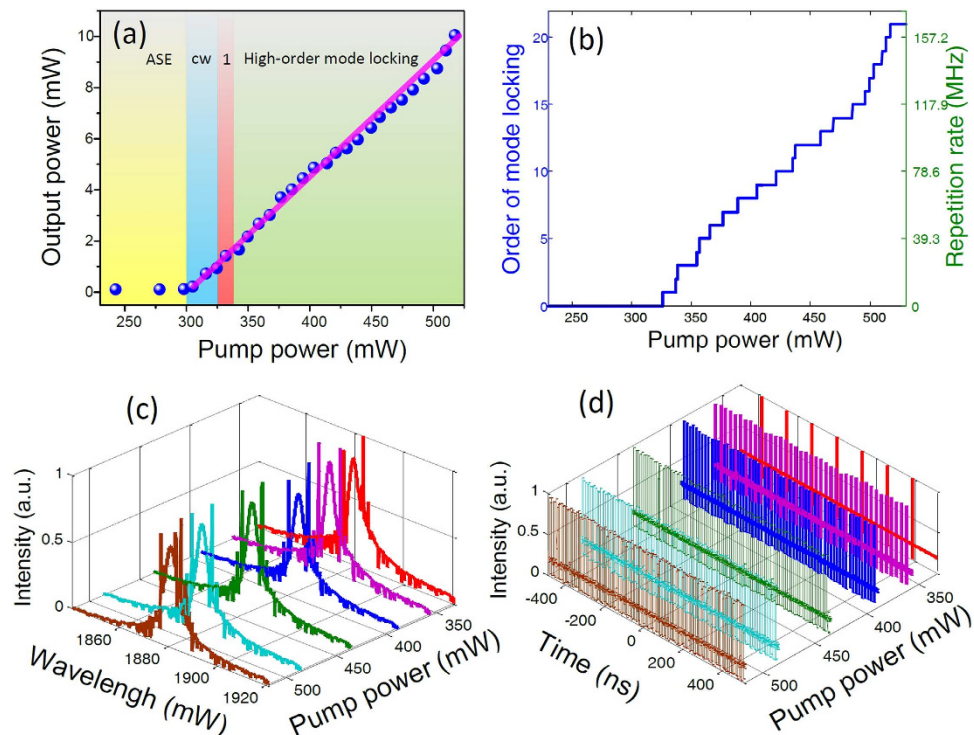


Figure 5. (a) The output power versus the pump power. Different color represents different operating regimes. (b) The repetition rate and orders of mode locking versus the pump power. The fundamental repetition rate to 21th harmonics mode-locking evolution versus the pump power, (c) the spectral evolution, (d) corresponding pulse train evolution.

The absorber structure in our work is quite different from those with the sandwich structure. In our work, higher-order harmonic mode locking is observed till to the 21th harmonic, which is limited by the damaged threshold of the WDM coupler rather than the absorber. The absorber with a sandwich structure, however, cannot bear such high pump power. Thus, it is difficult to observe higher-order harmonics mode locking based on the sandwich-structure absorber.

To increase the output power of our graphene based fiber laser, we use a home-made TDFA to amplify the seed laser. The maximum output power after amplification is ~450 mW by removing the residual pump power, when the passively mode-locked fiber oscillator operates at the fundamental mode locking (output power of the oscillator is 3 mW). The amplification coefficient is more than 21 dB. The spectral evolution at different output power is shown in Fig. 6(a). The spectra becomes broadening with the increase of the pump power. When the pump power is larger than 800 mW, the spectra are split and additional frequency components will generate as seen from the spectra. With further increasing the pump power of the TDFA, the spectra are broadened. More pair of humps will be generated in the frequency domain, which is due to the high nonlinear effect (such as modulation instability, self-phase modulation effect, etc). Simultaneously, the pulse will experience compressed processing, and multiple pulses process. Figure 6(b) shows the pulse evolution with the increase of the pump power. The pulse is compressed when the pump power increases. When the pump power is above 800 mW, the pulses become high order soliton pulses. More additional pulses can be generated with the increase of pump power. Figure 6(c) summarizes the spectral width and pulse-width evolution versus the pump power. We can see that below 800-mW pump power, the pulse becomes narrow and the spectra become broaden. Due to high-order nonlinear effect, the pulse is split into multiple pulses. With further increasing the pump power, more side humps are generated in the spectrum and additional sub-pulses are generated beside the main large pulse. Figure 6(d) shows the output power and the peak power versus the pump power of TDFA. We can see that the peak power becomes large with the increase of pump power. When the pump power is 800 mW, the peak power and average output power are 9.23 kW, 103.5 mW, respectively. By further increasing the pump power, high order soliton effect will make the pulse split into a main pulse and more sub pulses. In order to calculate the average peak power of the high-order soliton pulse, we assume the pulse width as the envelope width. The envelope width becomes wider because of high order-soliton pulse effect. When the pump power increases to 2 W, the output power is 456 mW. The peak power is estimated to be around 9.7 kW.

Conventionally, chirped pulse amplification (CPA) technique can overcome the pulse break-up, which is widely used in the normal-dispersion regime. After being amplified, the pulse can be further

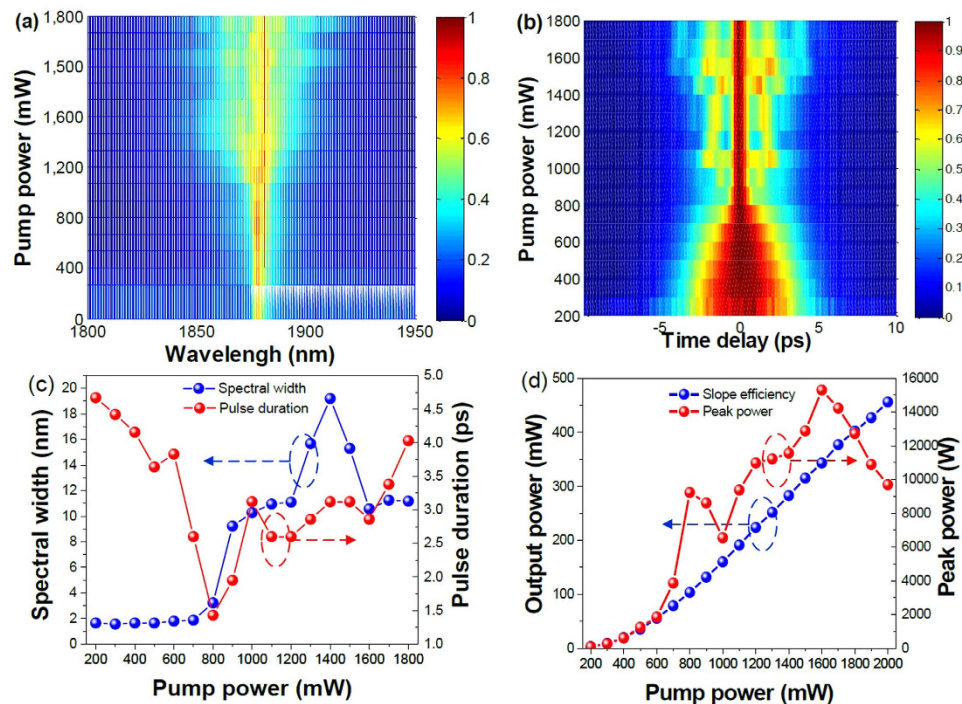


Figure 6. (a) The spectral evolution, (b) corresponding pulse evolution, (c) spectral width and pulse duration, (d) the output power and peak power versus the pump strength.

compressed due to the linear chirp of the pulse. Different from the CPA technique, the pulse can be amplified and compressed simultaneously in the anomalous dispersion regime. This can help to get shorter pulse than the transform-limited pulse due to the nonlinearity and high order soliton effect. Our approach provides a scheme to further compress the transform-limited pulse.

In order to demonstrate that the mode locking is solely mode locked by the SLG SA with graphene, we remove the side polished fiber with graphene or just remove the graphene on the side-polished fiber. No clear mode-locked pulse train or typical mode-locked spectrum can be observed. Only the CW regime was obtained from the laser cavity, which confirms that the mode locking is solely contributed by the side-polished fiber with graphene. The stability of our laser has been tested for a few days, no performance degradation was observed.

In conclusion, we demonstrate passively mode-locked high power Tm/Ho Co-doped fiber laser based on a side-polished fiber incorporated with CVD grown graphene. The obtained pulse width is about 4.7 ps, the spectral width is about 1.8 nm with Kerr side band, indicating that the fiber laser operates in the conventional soliton regimes. With further increase of the pump power, the Tm/Ho co-doped mode-locked fiber laser can operate in high-order harmonic mode locked states till to the 21th order, which is limited by the damaged threshold of fiber components. The output power of the proposed fiber laser can be further amplified to more than 450 mW, corresponding to a peak power of about 9.7 kW. The high peak-power Tm/Ho co-doped mode-locked fiber laser, with single mode output and high beam quality, can be potentially applied with further development in applications such as laser surgery, medical diagnostics, and gas detection, etc.

Method

Measurement method. Output spectra of our fiber lasers are measured through an optical spectrum analyzer (OSA, Yokogawa AQ6375). Mode-locked pulse train and radio frequency (RF) spectra are detected by using a 33-GHz mixed signal oscilloscope (MSO, Tektronix, 73304DX), one signal source analyzer (SSA, Rohde & Schwarz FSUP26) coupled with 12-GHz photodetector (Newport 818-BB-51F), respectively. A wide-range autocorrelator (From Femtochrome FR-103HP) is used to detect output pulse width.

References

- Li, X. *et al.* Broadband saturable absorption of graphene oxide thin film and its application in pulsed fiber lasers. *IEEE J Sel Top Quantum Electron* **20**, 1101107 (2014).
- Jackson, S. D. Towards high-power mid-infrared emission from a fibre laser. *Nat Photon* **6**, 423–431 (2012).
- Sorokina, I. T., Dvoynin, V. V., Tolstik, N. & Sorokin, E. Mid-IR ultrashort pulsed fiber-based lasers. *Selected Topics in Quantum Electronics, IEEE Journal of* **20**, 0903412 (2014).
- Liu, J., Shi, H., Liu, K., Tan, F. & Wang, P. in *Advanced Solid State Lasers*. AW4A.5 (Optical Society of America).

5. Matsas, V. J., Newson, T. P., Richardson, D. J. & Payne, D. N. Selfstarting passively mode-locked fibre ring soliton laser exploiting nonlinear polarisation rotation. *Electronics Letters* **28**, 1391–1393 (1992).
6. Li, X. H. *et al.* All-normal dispersion, figure-eight, tunable passively mode-locked fiber laser with an invisible and changeable intracavity bandpass filter. *Laser Phys* **21**, 940–944 (2011).
7. Fedotov, Y. S., Ivanenko, A. V., Kobtsev, S. M. & Smirnov, S. V. High average power mode-locked figure-eight Yb fibre master oscillator. *Opt Express* **22**, 31379–31386 (2014).
8. Duling, I. N., III, Chen, C. J., Wai, P. K. A. & Menyuk, C. R. Operation of a nonlinear loop mirror in a laser cavity. *Quantum Electronics, IEEE Journal of* **30**, 194–199 (1994).
9. Keller, U. *et al.* Semiconductor saturable absorber mirrors (SESAM's) for femtosecond to nanosecond pulse generation in solid-state lasers. *Selected Topics in Quantum Electronics, IEEE Journal of* **2**, 435–453 (1996).
10. Keller, U. Recent developments in compact ultrafast lasers. *Nature* **424** (2003).
11. Wang, F. Q. *et al.* Wideband-tunable, nanotube mode-locked, fibre laser. *Nat Nanotech* **3**, 738–742 (2008).
12. Sun, Z. P. *et al.* A stable, wideband tunable, near transform-limited, graphene-mode-locked, ultrafast laser. *Nano Research* **3**, 653–660 (2010).
13. Novoselov, K. S. *et al.* A roadmap for graphene. *Nature* **490**, 192–200 (2012).
14. Loh, K. P., Bao, Q. L., Eda, G. & Chhowalla, M. Graphene oxide as a chemically tunable platform for optical applications *Nat Chem* **2**, 1015–1024 (2010).
15. Zhang, Y. Z. *et al.* Broadband high photoresponse from pure monolayer graphene photodetector. *Nat Commun* **4**, 1811 (2013).
16. Mou, C. *et al.* Poor fluorinated graphene sheets carboxymethylcellulose polymer composite mode locker for erbium doped fiber laser. *Appl Phys Lett* **106**, 061106 (2015).
17. Hasan, T. *et al.* Nanotube–Polymer Composites for Ultrafast Photonics. *Adv Mater* **21**, 3874–3899 (2009).
18. Bao, Q. L. *et al.* Atomic-Layer Graphene as a Saturable Absorber for Ultrafast Pulsed Lasers. *Adv Funct Mater* **19**, 3077–3083 (2009).
19. Sun, Z. P. *et al.* Graphene Mode-Locked Ultrafast Laser. *ACS Nano* **4**, 803–810 (2010).
20. Martinez, A. & Sun, Z. P. Nanotube and graphene saturable absorbers for fibre lasers. *Nat Photonics* **7**, 842–845 (2013).
21. Sun, Z. P., Hasan, T. & Ferrari, A. C. Ultrafast lasers mode-locked by nanotubes and graphene. *Physica E Low Dimens Syst Nanostruct* **44**, 1082–1091 (2012).
22. Zhang, H. *et al.* Compact graphene mode-locked wavelength-tunable erbium-doped fiber lasers: from all anomalous dispersion to all normal dispersion. *Laser Phys Lett* **7**, 591 (2010).
23. Bonaccorso, F., Sun, Z., Hasan, T. & Ferrari, A. C. Graphene photonics and optoelectronics. *Nat Photonics* **4**, 611–622 (2010).
24. Hernandez, Y. *et al.* High-yield production of graphene by liquid-phase exfoliation of graphite. *Nat Nano* **3**, 563–568 (2008).
25. Li, X. *et al.* Large-Area Synthesis of High-Quality and Uniform Graphene Films on Copper Foils. *Science* **324**, 1312–1314 (2009).
26. Bae, S. *et al.* Roll-to-roll production of 30-inch graphene films for transparent electrodes. *Nat Nanotech* **5**, 574–578 (2010).
27. Sutter, P. W., Flege, J.-I. & Sutter, E. A. Epitaxial graphene on ruthenium. *Nat Mater* **7**, 406–411 (2008).
28. Wu, J., Pisula, W. & Müllen, K. Graphenes as Potential Material for Electronics. *Chemical Reviews* **107**, 718–747 (2007).
29. Zhang, H., Bao, Q., Tang, D., Zhao, L. & Loh, K. Large energy soliton erbium-doped fiber laser with a graphene-polymer composite mode locker. *Appl Phys Lett* **95**, 141103 (2009).
30. Tang, Y., Yu, X., Li, X., Yan, Z. & Wang, Q. J. High-power thulium fiber laser Q switched with single-layer graphene. *Opt Lett* **39**, 614–617 (2014).
31. Jung, M. *et al.* Mode-locked pulse generation from an all-fiberized, Tm-Ho-codoped fiber laser incorporating a graphene oxide-deposited side-polished fiber. *Opt Express* **21**, 20062–20072 (2013).
32. Tobben, H. Room temperature CW fibre laser at 3.5 μm in Er³⁺-doped ZBLAN glass. *Electronics Letters* **28**, 1361–1362 (1992).
33. Schneider, J., Carbonnier, C. & Unrau, U. B. Characterization of a Ho³⁺-doped fluoride fiber laser with a 3.9- μm emission wavelength. *Appl. Opt.* **36**, 8595–8600 (1997).
34. Zhang, M. *et al.* Tm-doped fiber laser mode-locked by graphene-polymer composite. *Opt Express* **20**, 25077–25084 (2012).
35. Sobon, G. *et al.* All-polarization maintaining, graphene-based femtosecond Tm-doped all-fiber laser. *Opt Express* **23**, 9339–9346 (2015).
36. Sotor, J. *et al.* Passive synchronization of erbium and thulium doped fiber mode-locked lasers enhanced by common graphene saturable absorber. *Opt Express* **22**, 5536–5543 (2014).
37. Wang, Q. *et al.* All-fiber passively mode-locked thulium-doped fiber ring laser using optically deposited graphene saturable absorbers. *Appl Phys Lett* **102**, 131117 (2013).
38. Fu, B. *et al.* Broadband Graphene Saturable Absorber for Pulsed Fiber Lasers at 1, 1.5 and 2 μm . *Selected Topics in Quantum Electronics, IEEE Journal of* **20**, 1100705 (2014).
39. Bo, F. *et al.* Generation of 35-nJ Nanosecond Pulse From a Passively Mode-Locked Tm, Ho-Codoped Fiber Laser With Graphene Saturable Absorber. *IEEE Photon. Technol. Lett.* **25**, 1447–1449 (2013).
40. Ferrari, A. C. *et al.* Raman Spectrum of Graphene and Graphene Layers. *Phys Rev Lett* **97**, 187401 (2006).
41. Das, A. *et al.* Monitoring dopants by Raman scattering in an electrochemically top-gated graphene transistor. *Nat Nano* **3**, 210–215 (2008).
42. Liu, X. *et al.* Multistability evolution and hysteresis phenomena of dissipative solitons in a passively mode-locked fiber laser with large normal cavity dispersion. *Opt Express* **17**, 8506–8512 (2009).
43. Adikan, F. R. M., Noor, A. S. M. & Mahdi, M. A. Optimum pumping configuration for L-band EDFA incorporating ASE pump source. *IEEE Photon. Technol. Lett.* **16**, 1465–1467 (2004).
44. Tang, D. Y., Zhao, L. M., Zhao, B. & Liu, A. Q. Mechanism of multisoliton formation and soliton energy quantization in passively mode-locked fiber lasers. *Phys Rev A* **72**, 043816 (2005).

Acknowledgements

We would like to acknowledge financial support from A*STAR SERC grant (Grant Number 112-290-4018), A*STAR SERC Advanced Optics in Engineering Programme (Grant no.: 122 360 0004), and A*STAR SERC Advanced Optics in Engineering Programme (Grant no.: 122 360 0011). This work is also partially funded by Teknologiateollisuus TT-100, Academy of Finland (No: 276376, 284548), the European Union's Seventh Framework Programme (REA grant agreement No: 631610), and Aalto University (Finland).

Author Contributions

X.L., Z.S. and Q.J.W. developed the ideas, proposed the laser system, performed the main experimental results, and wrote the manuscript. X.L. and X.Y. fabricated of the materials and measured the materials.

X.L., Z.S., X.Y., Y.Z., B.S. and Z.Y. discussed the performance of the system, materials, and considerably improved the manuscript presentation. All authors substantially contributed to the manuscript.

Additional Information

Competing financial interests: The authors declare no competing financial interests.

How to cite this article: Li, X. *et al.* High-power graphene mode-locked Tm/Ho co-doped fiber laser with evanescent field interaction. *Sci. Rep.* **5**, 16624; doi: 10.1038/srep16624 (2015).



This work is licensed under a Creative Commons Attribution 4.0 International License. The images or other third party material in this article are included in the article's Creative Commons license, unless indicated otherwise in the credit line; if the material is not included under the Creative Commons license, users will need to obtain permission from the license holder to reproduce the material. To view a copy of this license, visit <http://creativecommons.org/licenses/by/4.0/>